Article

SOURCE DATA | TRANSPARENT PROCESS | OPEN ACCESS

THE EMBO JOURNAL

Dephospho-CoA kinase, a nuclear-encoded apicoplast protein, remains active and essential after *Plasmodium falciparum* apicoplast disruption

Russell P Swift, Krithika Rajaram, Hans B Liu & Sean T Prigge*

Abstract

Malaria parasites contain an essential organelle called the apicoplast that houses metabolic pathways for fatty acid, heme, isoprenoid, and iron–sulfur cluster synthesis. Surprisingly, malaria parasites can survive without the apicoplast as long as the isoprenoid precursor isopentenyl pyrophosphate (IPP) is supplemented in the growth medium, making it appear that isoprenoid synthesis is the only essential function of the organelle in blood-stage parasites. In the work described here, we localized an enzyme responsible for coenzyme A synthesis, DPCK, to the apicoplast, but we were unable to delete DPCK, even in the presence of IPP. However, once the endogenous DPCK was complemented with the *E. coli* DPCK (*Ec*DPCK), we were successful in deleting it. We were then able to show that DPCK activity is required for parasite survival through knockdown of the complemented *Ec*DPCK. Additionally, we showed that DPCK enzyme activity remains functional and essential within the vesicles present after apicoplast disruption. These results demonstrate that while the apicoplast of blood-stage *P. falciparum* parasites can be disrupted, the resulting vesicles remain biochemically active and are capable of fulfilling essential functions.

Keywords apicoplast; coenzyme A; DPCK; malaria; *Plasmodium falciparum*
Subject Categories Metabolism; Microbiology, Virology & Host Pathogen Interaction
DOI 10.15252/embj.2020107247 | Received 6 November 2020 | Revised 6 April 2021 | Accepted 26 April 2021 | Published online 25 May 2021
The EMBO Journal (2021) 40: e107247

Introduction

Plasmodium falciparum parasites rely on exogenous pantothenate (vitamin B5) (Geary *et al,* 1985; Saliba *et al,* 2005), which they use for the *de novo* synthesis of coenzyme A (CoA) (Spry & Saliba, 2009). Within the parasite, CoA functions as an essential cofactor that is used for a variety of biosynthetic pathways (Spry *et al,* 2008), including the generation of acetyl-CoA, fatty acid biosynthesis and modification, and cellular oxidation and metabolism (Spry *et al,* 2010). The CoA biosynthetic pathway has been considered as an attractive source of antimalarial drug targets, with multiple studies showing that inhibitors of this pathway are effective against the asexual red blood cell (RBC) stage of the parasite (Spry *et al,* 2005; Spry *et al,* 2013; Macuamule *et al,* 2015; Schalkwijk *et al,* 2019).

Pantothenate is imported into malaria parasites by a proton-coupled pantothenate transporter (Saliba & Kirk, 2001). In *P. falciparum*, the transporter PAT (PF3D7_0206200) has been proposed to fulfill this role (Augagneur *et al,* 2013). However, there is some uncertainty about the exact function of PAT since it is dispensable in blood-stage parasites and appears to be essential for processes such as exocytosis and vesicle fusion during other stages of parasite development (Hart *et al,* 2014; Kehrer *et al,* 2016; Kenthirapalan *et al,* 2016). Once inside the cell, pantothenate is converted into CoA through a series of five enzyme-mediated steps (Saliba & Kirk, 2001; Hart *et al,* 2014). The first four enzymes, including pantothenate kinase 1 or 2 (PanK1/2), phosphopantothenoylcysteine synthase 1 or 2 (PPCS1/2), phosphopantothenoylcysteine decarboxylase (PPCDC), and phosphopantetheine adenylyltransferase (PPAT), are believed to localize to the cytosol of the parasite (Spry *et al,* 2008). However, the last step of this pathway, in which dephospho-CoA kinase (DPCK) converts dephospho-CoA to CoA, is predicted to occur within the apicoplast (Fig 1) (Ralph *et al,* 2004).

While not experimentally confirmed, DPCK is predicted to localize to the apicoplast due to the presence of an N-terminal bipartite apicoplast trafficking peptide (Ralph *et al,* 2004). The CoA generated by DPCK is thought to be used within the apicoplast to modify the acyl-carrier protein (ACP) with a 4-phosphopantetheine cofactor (Spry *et al,* 2008). This modification is catalyzed by ACP synthase (ACPS) and is required to form the mature and biologically active form of ACP, holo-ACP (Waters *et al,* 2002; Spry *et al,* 2008; Gallagher & Prigge, 2010). Holo-ACP plays a central role in the type II fatty acid synthesis (FASII) pathway within the apicoplast (Ralph *et al,* 2004; Shears *et al,* 2015). Additionally, since DPCK provides the only predicted source of CoA for the parasite, the CoA generated within the apicoplast is presumably exported out of the organelle for use throughout the parasite cell by a transporter that has yet to be identified (Spry *et al,* 2008).

It has previously been demonstrated that the apicoplast organelle can be disrupted in blood-stage *P. falciparum* parasites if supplemented with sufficient levels of the isoprenoid precursor isopentenyl

Department of Molecular Microbiology and Immunology, Johns Hopkins Bloomberg School of Public Health, Baltimore, MD, USA
*Corresponding author. Tel: +1 443 287 4822; E-mail: sprigge2@jhu.edu

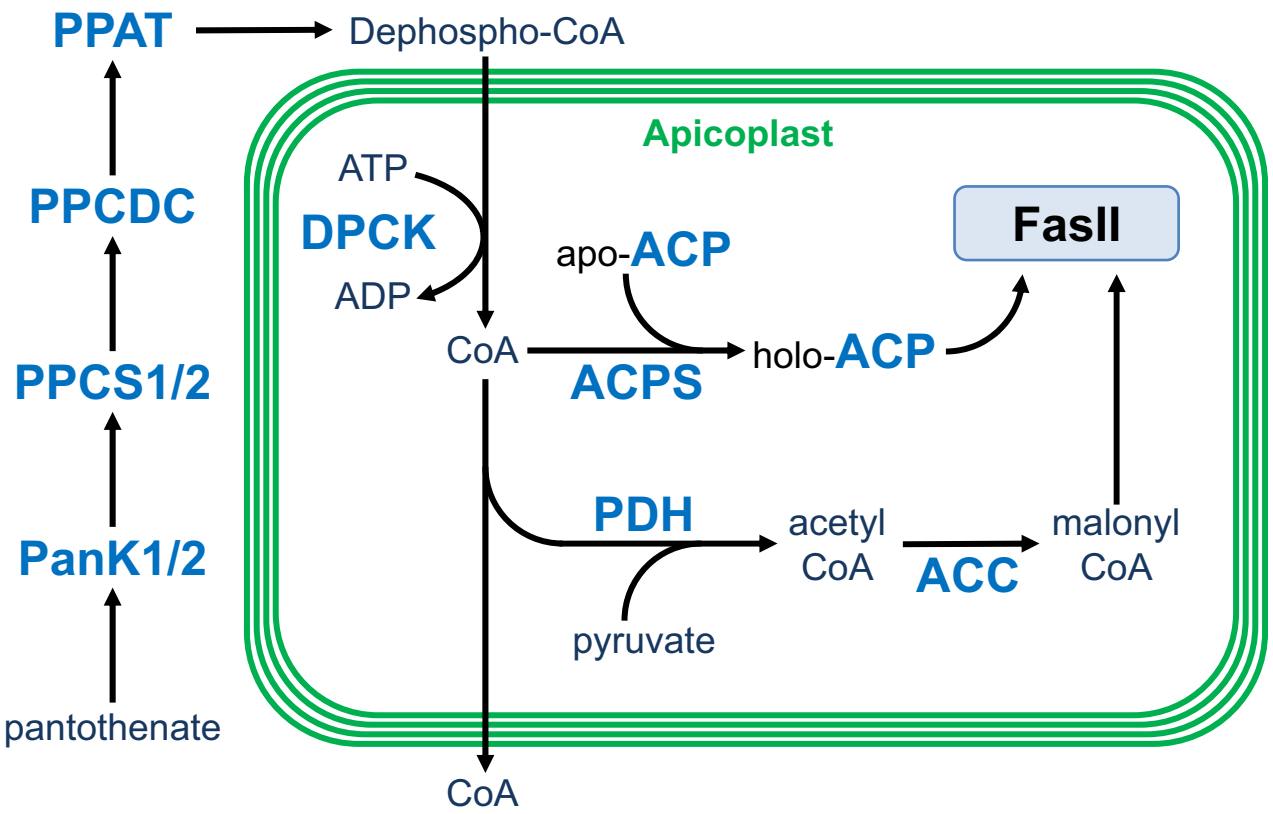

Figure 1. Generation of CoA and its utilization in the apicoplast.

Pantothenate is metabolized into dephospho-CoA through a series of enzymes within the cytosol (PanK1/2, PPCS1/2, PPCDC, and PPAT). The final step involves the generation of CoA by DPCK and is believed to occur within the apicoplast. Within the apicoplast, CoA is used to generate acetyl-CoA and malonyl-CoA and is used by ACPS to carry out the 4-phosphopantetheine modification of ACP to generate holo-ACP. The CoA produced within the apicoplast is also believed to be exported into the cytosol for utilization throughout the parasite cell. PanK1/2: pantothenate kinase 1 or 2; PPCS1/2: phosphopantothenoylcysteine synthase 1 or 2; PPCDC: phosphopantothenoylcysteine decarboxylase; PPAT: phosphopantetheine adenylyltransferase; DPCK: dephospho-CoA kinase; ACP: acyl-carrier protein; ACPS: acyl-carrier protein synthase; ACC: acetyl-CoA carboxylase; PDH: pyruvate dehydrogenase.

pyrophosphate (IPP) (Yeh & DeRisi, 2011). These results have been interpreted as IPP being the only essential product of the apicoplast. However, with DPCK also predicted to be an essential apicoplast-localized protein, parasites containing a disrupted apicoplast should then require supplementation with both CoA and IPP to survive (Ralph *et al,* 2004; Hart *et al,* 2017). The ability of parasites to survive on IPP supplementation alone may be explained by the finding that parasites with a disrupted apicoplast have been shown to accumulate vesicles throughout the cell (Yeh & DeRisi, 2011; Gisselberg *et al,* 2013). These vesicles contain nuclear-encoded apicoplast-specific proteins that would have presumably been trafficked to the organelle under typical conditions (Bowman *et al,* 2014; Pasaje *et al,* 2016; Florentin *et al,* 2017; Uddin *et al,* 2018). Thus, it is possible that vesicle-localized proteins remain biochemically active and are capable of fulfilling their essential functions within the cell.

Through the work described here, we confirmed the apicoplast localization of DPCK. Additionally, we attempted to generate a genetic knockout of DPCK and were unsuccessful, even with an apicoplast metabolic bypass, suggesting an essential role beyond its function within the organelle. However, upon complementation of the endogenous DPCK with *E. coli* DPCK (*Ec*DPCK), we were successful in deleting it. This not only helps to confirm the activity of the endogenous DPCK, which has not been previously enzymatically characterized, but also provides additional evidence that the protein is likely to be essential. To demonstrate that DPCK activity is indeed essential, we knocked down the complemented *Ec*DPCK in a parasite line in which the endogenous DPCK had been deleted, which resulted in the inhibition of parasite growth. We also showed that DPCK is present and active in the parasite vesicles that are generated after the disruption of the apicoplast, with that activity being required for parasite growth. Overall, these results demonstrate that the vesicles generated after the disruption of the apicoplast in blood-stage *P. falciparum* parasites remain biochemically active and capable of fulfilling essential metabolic functions.

Results

DPCK is refractory to deletion, even when provided with a metabolic bypass

Based on the assumption that DPCK is an essential apicoplast protein, we attempted to delete it in a metabolic bypass parasite line

called PfMev. The PfMev line contains a genetically encoded apicoplast bypass system that can convert exogenously supplied mevalonate into the isoprenoid precursors isopentenyl pyrophosphate (IPP) and dimethylallyl pyrophosphate (DMAPP) (Swift *et al,* 2020b). In the presence of mevalonate, PfMev parasites can survive the deletion of essential apicoplast proteins and even the disruption of the apicoplast organelle (Swift *et al,* 2020a; Swift *et al,* 2020b). The PfMev parasite line also expresses the green fluorescent protein, super-folder green (SFG), with the N-terminal trafficking peptide of the *P. falciparum* acyl-carrier protein (api-SFG), which directs its trafficking to the apicoplast, thereby fluorescently labeling the organelle (Swift *et al,* 2020b).

Using the PfMev line, we attempted to delete DPCK using Cas9-mediated genome editing (Ghorbal *et al,* 2014), under continuous supplementation with 50 μM mevalonate. This should allow DPCK to be deleted even if it is required for apicoplast function. However, we failed to delete DPCK despite six independent attempts (Appendix Table S1). Two of these attempts were done with direct supplementation of 5 mM CoA, which has been shown to rescue the growth of parasites treated with inhibitors that target the CoA biosynthetic pathway (Spry *et al,* 2010; Fletcher & Avery, 2014; Fletcher *et al,* 2016). As discussed further below, this result is consistent with the hypothesis that CoA supplementation may only bypass early steps of the CoA biosynthesis pathway. The inability to delete DPCK in the presence of mevalonate suggests that DPCK has an essential function beyond its potential requirement within the apicoplast or that it is not actually an apicoplast protein to begin with.

DPCK localizes to the apicoplast organelle

In *P. falciparum,* DPCK is predicted to localize to the apicoplast (Ralph *et al,* 2004), but this has yet to be experimentally confirmed. In order to determine the localization of DPCK, we generated a genetic construct for the expression of DPCK with a C-terminal mCherry tag under control of the calmodulin promoter and integrated it into the genome of PfMev parasites. To accomplish this, we first inserted an attB site into a locus known to be dispensable in blood-stage parasites (P230p; PF3D7_0208900) (Marin-Mogollon *et al,* 2018). Plasmids pCasG (Rajaram *et al,* 2020) and pRS (Swift *et al,* 2020b) were used to insert the 40 base pair attB sequence using markerless selection (Figs 2A and EV1) followed by sequencing to verify the correct insertion. The resulting PfMev p230p attB line was used for this, and all subsequent experiments, unless otherwise noted. The DPCK-mCherry expression construct was inserted into this line using attP/attB recombination (Nkrumah *et al,* 2006; Spalding *et al,* 2010) and verified with genotyping PCRs (Figs 2B and EV2A). Analysis via live epifluorescence microscopy revealed colocalization of the api-SFG and mCherry signals, indicating that DPCK is indeed located in the apicoplast (Fig 2C, Table 1).

DPCK deletion is enabled by apicoplast complementation with *E. coli* DPCK, which is present and active within disrupted apicoplast vesicles

Since we failed to knockout DPCK directly, we attempted to delete DPCK in parasites complemented with the *E. coli* DPCK (*Ec*DPCK) in

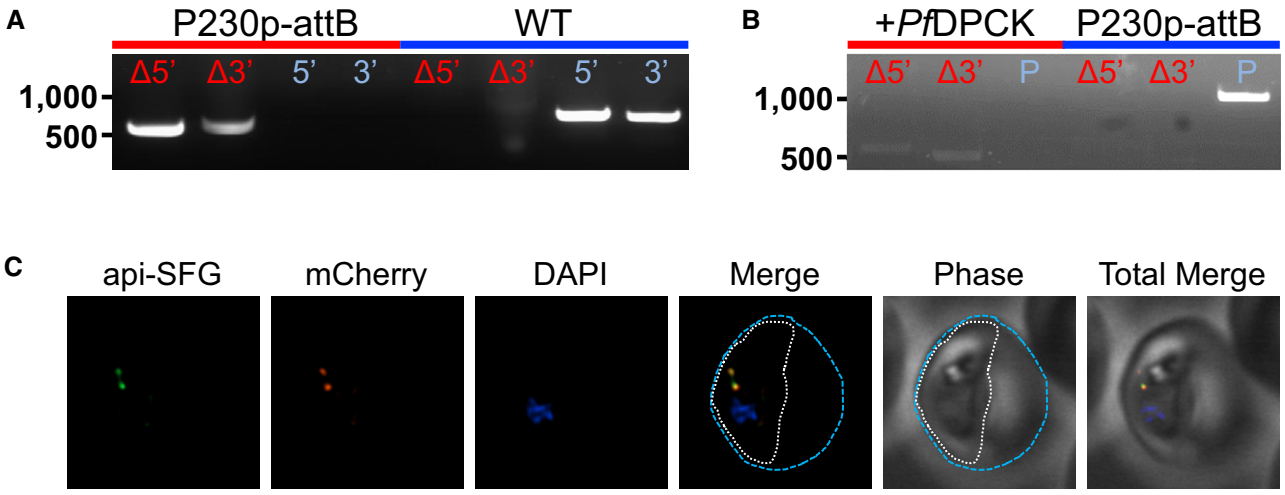

Figure 2. Colocalization of DPCK-mCherry with the apicoplast marker api-SFG.

A Genotyping PCR confirming the insertion of a 40 bp attB element in the *p230p* gene, with amplification demonstrating integration at the Δ5' and Δ3' loci and lack of wild-type parasites (as indicated by the failure to amplify at the wild-type 5' and 3' loci) as compared to the parental control. A schematic describing these genotyping PCRs is shown in Fig EV1.

B Genotyping PCR confirming the insertion of the *Pf*DPCK-mCherry construct using attP/attB integration. PCRs demonstrate integration at the Δ5' and Δ3' integration sites and lack of parental parasites (P) as compared to the parental control (P230p-attB). A schematic describing these genotyping PCRs is shown in Fig EV2A.

C Live epifluorescence microscopy of PfMev parasites that are expressing api-SFG (green) and the *P. falciparum* DPCK-mCherry protein (red) with DAPI marking the nuclei (blue). Colocalization statistics are shown in Table 1. The borders of the red blood cell and parasite are marked with dotted blue and white lines, respectively. Microscopy images represent fields that are 10 μm long by 10 μm wide.

Source data are available online for this figure.

Table 1. Colocalization Manders M2 values for parasite lines with different treatments.

Parasite Line	Treatment	M2	SEM	N	Figure
PfDPCK-mCherry	none	**0.62**	0.04	31	2C
api-EcDPCK-mCherry	none	**0.78**	0.03	6	3C
api-EcDPCK-mCherry	Δ*dpck*	**0.72**	0.03	62	3D
api-EcDPCK-mCherry	Δ*dpck*, Azith	**0.73**	0.02	50	3E
EcDPCK-mCherry	none	0.17	0.03	18	4A
EcDPCK-mCherry	Δ*dpck*	0.15	0.01	40	4B
CLD-EcDPCK-mCherry-apt	aTc	**0.71**	0.05	14	
CLD-EcDPCK-mCherry-apt	Δ*dpck*, aTc	**0.74**	0.02	45	5C
CLD-EcDPCK-mCherry-apt	Δ*dpck*	*0.04	0.00	18	5D
CLD-EcDPCK-mCherry-apt	Δ*dpck*, aTc, Shield1	0.18	0.02	27	5E
CLD-EcDPCK-mCherry-apt	Δ*dpck*, Shield1	*0.02	0.01	11	5F

The Manders M2 value is shown for the colocalization of different DPCK constructs with apicoplast-localized SFG. The standard error of the mean (SEM), total number of observations (N), and corresponding figure numbers are shown. M2 values indicating apicoplast localization are in bold. Asterisks mark values calculated with very low fluorescence signal due to knockdown of the mCherry fusion protein.

the apicoplast. We generated an expression construct containing the *Ec*DPCK with the signal and transit peptide of the *P. falciparum* ACP appended to the N-terminus to direct its trafficking to the apicoplast (Waller *et al,* 2000), in addition to a C-terminal mCherry tag for localization (Fig 3A). The expression of this gene was controlled by the calmodulin promoter, and the construct was integrated into the genome of the PfMev P230p attB parasite line using attP/attB integration (Nkrumah *et al,* 2006; Spalding *et al,* 2010) and verified by PCR (Fig EV2A and B). Analysis of the PfMev api-*Ec*DPCK-mCherry line by live epifluorescence microscopy showed colocalization of the mCherry and api-SFG signals, demonstrating that the *E. coli* DPCK was being expressed and trafficked to the apicoplast (Fig 3B, Table 1). In this parasite line, we successfully deleted the endogenous DPCK and confirmed the deletion via PCR (Figs 3C and EV3). After deleting the endogenous DPCK, we analyzed the resulting PfMev api-*Ec*DPCK-mCherry Δ*dpck* line via live epifluorescence microscopy and confirmed that the api-SFG and mCherry signals continued to be colocalized in the apicoplast (Fig 3D, Table 1). These results indicate that apicoplast expression of *Ec*DPCK can complement the loss of the parasite DPCK and that DPCK is likely essential because it can only be deleted when complemented. Additionally, since the *E. coli* DPCK (encoded by the *coaE* gene) has already been biochemically characterized (Mishra *et al,* 2001), successful complementation indicates that the putative parasite DPCK (which has not previously been biochemically characterized) has dephospho-CoA kinase enzymatic activity.

We next wanted to determine whether apicoplast *Ec*DPCK expression could complement parasites containing a disrupted apicoplast. Continued parasite survival in this state would indicate that the *Ec*DPCK is present and active within the disrupted apicoplast vesicles. Thus, we treated the PfMev api-*Ec*DPCK-mCherry Δ*dpck* line with 100 nM azithromycin in the presence of 50 μM mevalonate for 7 days to induce apicoplast disruption (Gisselberg *et al,* 2013). The azithromycin-treated parasites continued to survive in media with added mevalonate, and analysis by live epifluorescence microscopy showed the presence of multiple vesicles instead of the typical intact organellar structure, consistent with the previously reported disruption phenotype (Yeh & DeRisi, 2011; Gisselberg *et al,* 2013). Furthermore, in this parasite line both the api-SFG and mCherry signals remained colocalized, indicating that *Ec*DPCK was present within the apicoplast vesicles of the parasite (Fig 3E, Table 1). We then confirmed apicoplast disruption using a PCR assay to demonstrate loss of the *sufB* gene (Gisselberg *et al,* 2013), encoded by the apicoplast genome (Fig 3F). Apicoplast disruption was also corroborated by Western blot analysis of api-*Ec*DPCK-mCherry and api-SFG, which revealed the presence of precursor and mature proteins in untreated parasites but only the precursor proteins in parasites exposed to azithromycin (Fig EV4). Taken together, in the presence of a disrupted apicoplast, the continued parasite survival and colocalization of the api-SFG and mCherry signals suggest that *Ec*DPCK is present and active within the vesicles present after apicoplast disruption.

DPCK can be knocked out if complemented with the *E. coli* DPCK in the cytosol

It is not clear why the last step of CoA synthesis occurs in the apicoplast. Within the apicoplast, CoA is used to form the 4'-phosphopantetheine prosthetic group found on ACP (Waters *et al,* 2002), which plays a central role in the FASII fatty acid biosynthetic pathway (Prigge *et al,* 2003). However, this pathway is dispensable in blood-stage parasites (Foth *et al,* 2005; van Schaijk *et al,* 2014). One would therefore expect the cytosolic expression of DPCK to be sufficient to complement blood-stage parasites, unless DPCK is required within the organelle for a separate and essential purpose. To investigate this, we generated a second complementation line expressing the *Ec*DPCK-mCherry protein lacking an N-terminal trafficking peptide, for cytosolic expression (Fig 4A). This construct was integrated into the PfMev p230p attB parasite line using attP/attB recombination (Nkrumah *et al,* 2006; Spalding *et al,* 2010) and verified by PCR (Fig EV2A and B). As expected, the cytosolic *Ec*DPCK-mCherry protein did not localize to the apicoplast (Fig 4B, Table 1) and Western blot analysis revealed a single band corresponding to the full-length protein (Fig EV4). We then used this parasite line to delete the endogenous DPCK under supplementation with 50 μM mevalonate (Fig 4C). Parasites were supplemented with mevalonate to bypass any potential essential DPCK activity within the apicoplast. Analysis of the resulting apicoplast phenotype revealed that the organelle remained intact (Fig 4D and E), and the parasites were not reliant on mevalonate supplementation for survival. Overall, these results indicate that cytosolic DPCK can provide CoA for all essential processes in blood-stage parasites.

DPCK activity is required for parasite growth

While the previous results strongly suggest that DPCK activity is required for parasite survival, in order to more conclusively

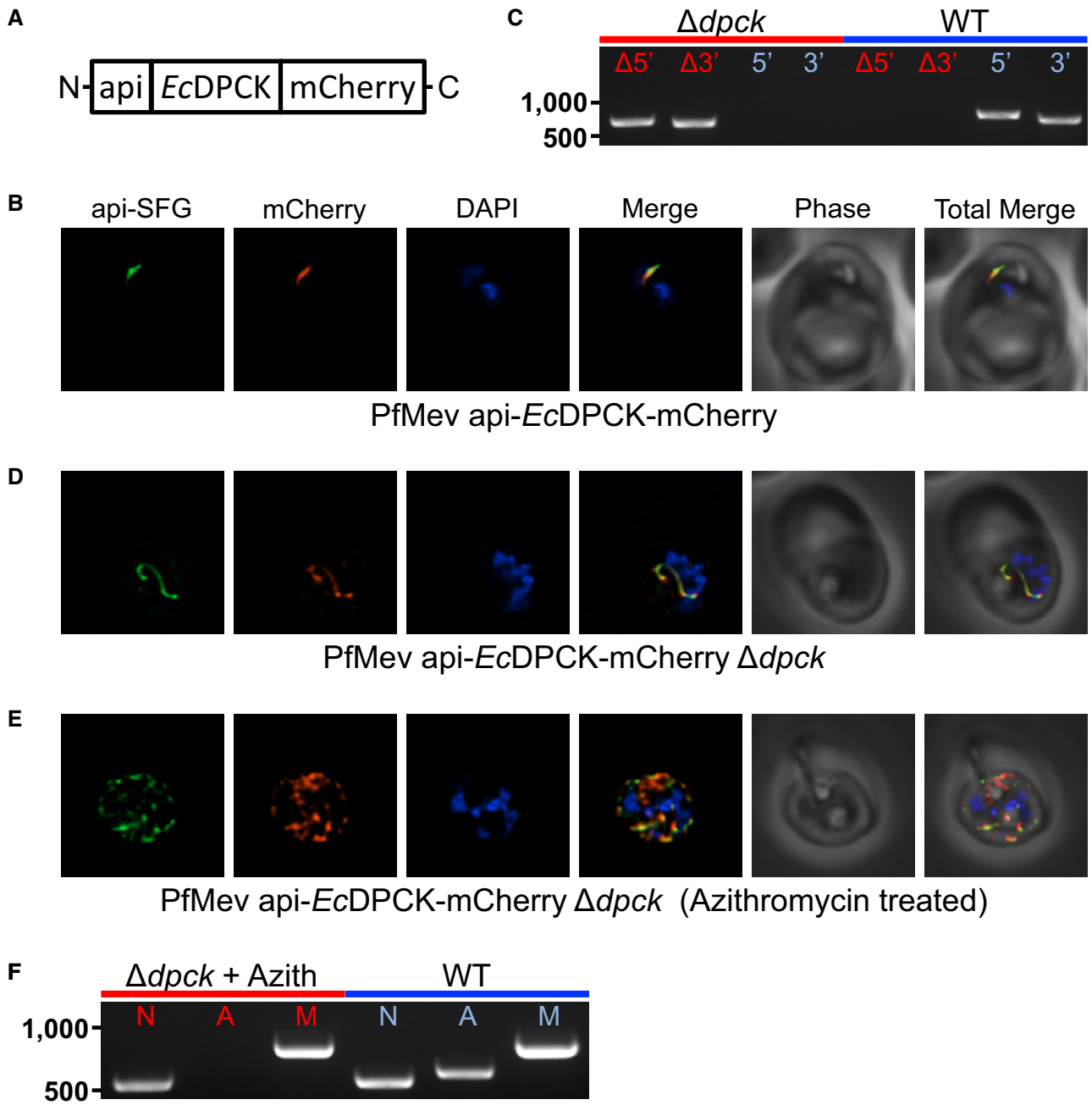

Figure 3. *E. coli* DPCK complementation in the apicoplast and the deletion of DPCK.

A Construct used to express the *E. coli* DPCK in the apicoplast. Appended are the N-terminal signal sequence and transit peptide from ACP (api) and a C-terminal mCherry tag.

B Live epifluorescence microscopy of PfMev parasites that are expressing api-SFG (green) and api-*Ec*DPCK-mCherry (red) with DAPI marking the nuclei (blue).

C Genotyping PCR confirming the deletion of the endogenous DPCK, with amplification demonstrating integration at the Δ5' and Δ3' loci and lack of wild-type parasites (as indicated by the failure to amplify at the wild-type 5' and 3' loci) as compared to the parental control. A schematic describing these genotyping PCRs is shown in Fig EV3.

D Live epifluorescence microscopy of the PfMev api-*Ec*DPCK-mCherry Δ*dpck* parasite line that is expressing api-SFG (green) and api-*Ec*DPCK-mCherry (red) with DAPI marking the nuclei (blue).

E Live epifluorescence microscopy of the PfMev api-*Ec*DPCK-mCherry Δ*dpck* line after treatment with 1x azithromycin for 7 days under supplementation with 50μM mevalonate. This parasite line expresses api-SFG (green) and api-*Ec*DPCK-mCherry (red) with DAPI marking the nuclei (blue).

F Attempted PCR detection of the *ldh*, *sufB*, and *cox1* genes from the nuclear (N), apicoplast (A), and mitochondrial (M) genomes, respectively. We failed to amplify *sufB* from the azithromycin-treated (+ Azith) PfMev api-*Ec*DPCK-mCherry Δ*dpck* parasites, indicating the loss of the apicoplast organellar genome.

Data information: All microscopy images represent fields that are 10 μm long by 10 μm wide. Colocalization statistics are shown in Table 1.
Source data are available online for this figure.

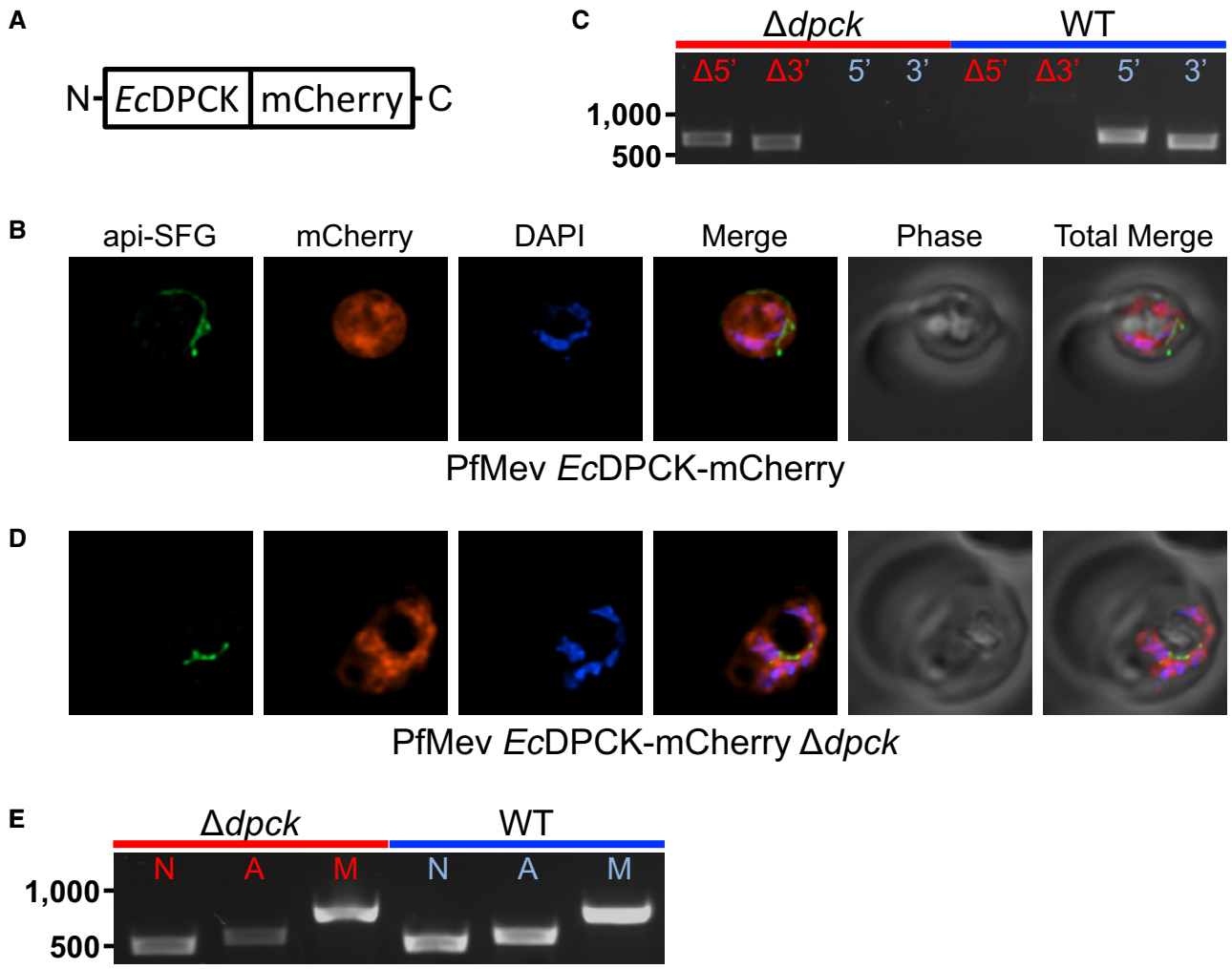

Figure 4. *E. coli* DPCK complementation in the cytosol and deletion of DPCK.

A Construct used to express the *E. coli* DPCK protein with a C-terminal mCherry tag in the cytosol of the PfMev parasite line.

B Live epifluorescence microscopy of the PfMev *Ec*DPCK-mCherry line. This parasite line expresses api-SFG (green) and *Ec*DPCK-mCherry (red) with DAPI marking the nuclei (blue).

C Genotyping PCR confirming the deletion of the endogenous DPCK using primer pairs described in Fig EV3.

D Live epifluorescence microscopy of the PfMev *Ec*DPCK-mCherry Δ*dpck* line. This parasite line expresses api-SFG (green) and *Ec*DPCK-mCherry (red) with DAPI marking the nuclei (blue).

E Attempted PCR detection of the *ldh*, *sufB*, and *cox1* genes from the nuclear (N), apicoplast (A), and mitochondrial (M) genomes, respectively. We were successful in amplifying *sufB* from the PfMev *Ec*DPCK-mCherry Δ*dpck* parasite line grown under continuous supplementation with 50μM mevalonate, indicating retention of the apicoplast organellar genome.

Data information: All microscopy images represent fields that are 10 μm long by 10 μm wide. Colocalization statistics are shown in Table 1.
Source data are available online for this figure.

demonstrate this, we attempted to knockdown the complemented *Ec*DPCK in parasites in which the endogenous DPCK had been deleted. The expression of *Ec*DPCK-mCherry was made controllable through the previously established tetR-DOZI system, which relies on a C-terminal aptamer array to inhibit translation upon the removal of anhydrotetracycline (aTc) from the parasite culture (Goldfless *et al,* 2014). Additionally, for a second form of inducible control of *Ec*DPCK, we appended an N-terminal conditional localization domain (CLD). The CLD directs protein trafficking to the apicoplast, but is rerouted and secreted into the parasitophorous vacuole upon the addition of the ligand Shield1 (Fig 5A) (Gallagher *et al,* 2011; Roberts *et al,* 2019). Both systems were simultaneously employed to ensure that we could achieve sufficient downregulation of *Ec*DPCK, which is expressed by the strong bidirectional calmodulin promoter (Crabb & Cowman, 1996; Epp *et al,* 2008). This construct was integrated into the PfMev p230p attB parasite line (Fig EV2A and B), followed by deletion of the endogenous DPCK, confirmed via PCR (Fig 5B), generating the resulting PfMev CLD-*Ec*DPCK-mCherry-apt (aptamer) Δ*dpck* parasite line. Expression and apicoplast trafficking of the CLD-*Ec*DPCK-mCherry protein were

confirmed via live epifluorescence microscopy (Fig 5C, Table 1). We then verified the functionality of the individual knockdown systems via live epifluorescence microscopy through the removal of aTc (Fig 5D), the addition of Shield1 (Fig 5E), or the simultaneous removal of aTc and the addition of Shield1 (Fig 5F). Removal of aTc resulted in a diminished mCherry signal, consistent with knockdown of the protein, and the addition of Shield1 resulted in mislocalization of the protein away from the apicoplast (Fig 5, Table 1).

In the non-permissive state for both systems (aTc removed, Shield1 added), we conducted an assay, tracking parasite growth over 6 days, and only observed a ~50% reduction in growth on day 6 (Appendix Fig S1). We reasoned that this mild growth inhibition may be due to incomplete knockdown of *Ec*DPCK, with high expression driven by the calmodulin promoter. Thus, to potentially exacerbate the observed growth phenotype, we limited the amount of exogenously provided pantothenate from the culture medium in order to sensitize the parasites to reduced levels of DPCK. While typical parasite media contains ~1 μM pantothenate, we found that as little as 50 nM was sufficient to allow parasites to grow at near wild-type levels (Fig EV5). This is consistent with previous work

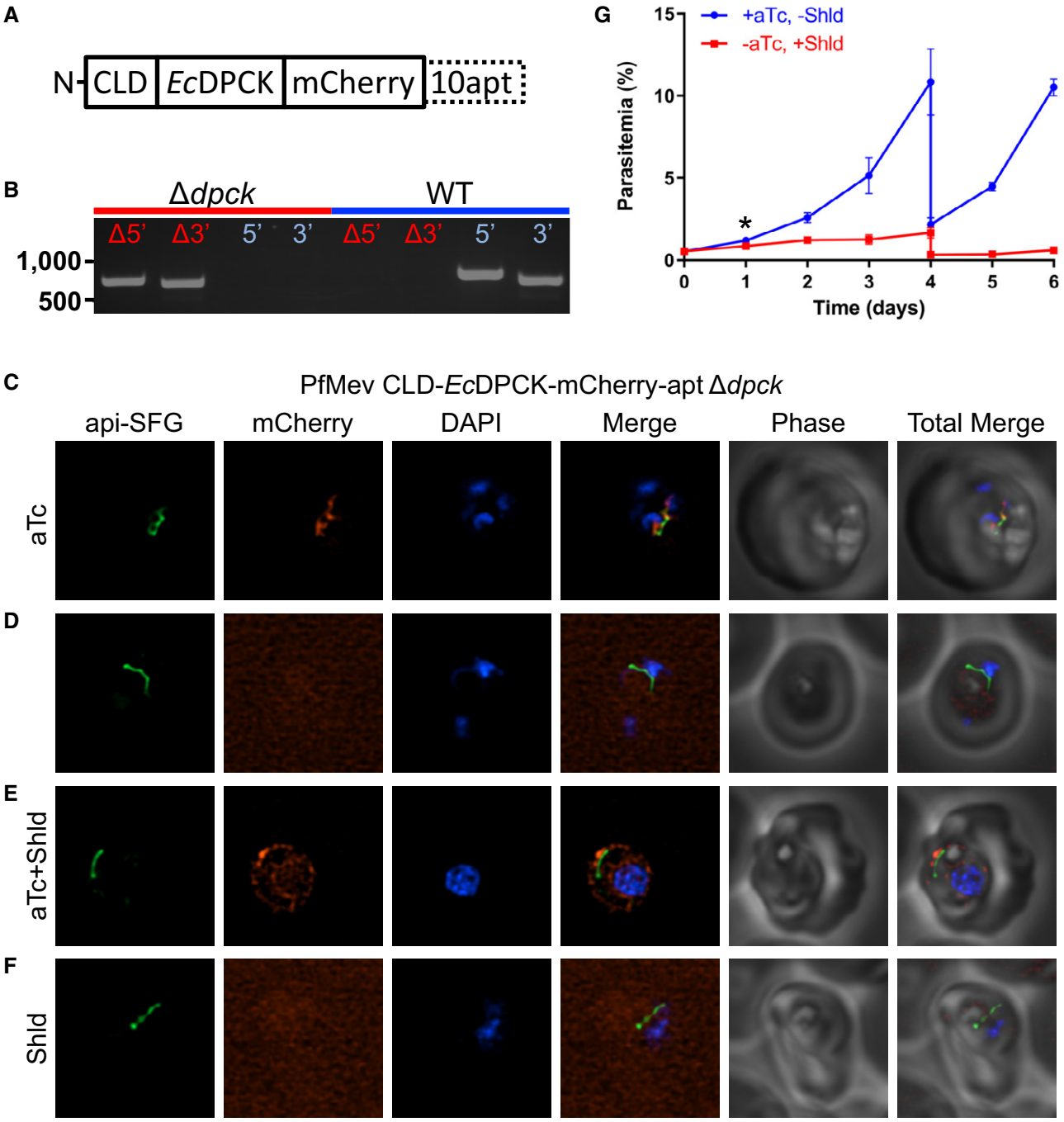

Figure 5.

Figure 5. Characterization of the PfMev CLD-*Ec*DPCK-mCherry-apt Δ*dpck* line under permissive and non-permissive conditions.

A Construct used to generate the PfMev CLD-*Ec*DPCK-mCherry-apt parasite line.
B Genotyping PCR confirming the deletion of the endogenous DPCK (Δ*dpck*) using primer pairs described in Fig EV3.
C Live epifluorescence microscopy of the PfMev CLD-*Ec*DPCK-mCherry-apt Δ*dpck* line. This parasite line expresses api-SFG (green) and CLD-*Ec*DPCK-mCherry (red) with DAPI marking the nuclei (blue). This parasite line was grown in the presence of 0.5 μM aTc.
D The PfMev CLD-*Ec*DPCK-mCherry-apt Δ*dpck* parasite line grown in the absence of aTc for 48 h. The brightness of the red fluorescence image was increased to demonstrate the lack of mCherry signal associated with the parasite.
E The PfMev CLD-*Ec*DPCK-mCherry-apt Δ*dpck* parasite line grown in the presence of 0.5 μM aTc and in the presence of 0.5 μM Shield1 (Shld) for 48 h.
F The PfMev CLD-*Ec*DPCK-mCherry-apt Δ*dpck* parasite line grown in the absence of aTc and in the presence of 0.5 μM Shield1 (Shld) for 48 h. The brightness of the red fluorescence image was increased to demonstrate the lack of mCherry signal associated with the parasite.
G Growth curve of the PfMev CLD-*Ec*DPCK-mCherry-apt Δ*dpck* parasite line grown either in the presence of 0.5 μM aTc and the absence 0.5 μM Shield1 (permissive condition, blue), or the absence of 0.5 μM aTc and the presence of 0.5 μM Shield1 (non-permissive condition, red). Pantothenate was supplied at 50 nM in both conditions, and the cultures were diluted 1:5 on day 4. Treatment under non-permissive conditions resulted in reduced parasite growth beginning at day 1 (two-way ANOVA, followed by Bonferroni's correction; $*P < 0.05$). Error bars represent the standard error of the mean from two independent experiments, each conducted in quadruplicate.

Data information: All microscopy images represent fields that are 10 μm long by 10 μm wide. Colocalization statistics are shown in Table 1.
Source data are available online for this figure.

which found the concentration of pantothenate required to support parasite growth at half the level of control parasites (SC_{50}) to be ~9.4 nM (Tjhin *et al,* 2018). Under limiting pantothenate concentrations, we observed a severe growth defect for the PfMev CLD-*Ec*DPCK-mCherry-apt Δ*dpck* parasite line under non-permissive conditions, indicating that DPCK activity is required for parasite growth (Fig 5G).

DPCK activity in disrupted apicoplast vesicles is essential for parasite growth

While the previous results demonstrated that DPCK activity is essential, it is not clear whether disrupted apicoplast vesicles remain biochemically active and if DPCK activity remains functional within these vesicles. To help elucidate this, we induced apicoplast disruption in the PfMev CLD-*Ec*DPCK-mCherry-apt Δ*dpck* line by treating the parasites with 100 nM azithromycin in the presence of 50 μM mevalonate for 7 days, with organelle disruption confirmed via PCR and epifluorescence microscopy (Fig 6A and B). We observed by microscopy that the api-SFG and mCherry signals colocalized, indicating that *Ec*DPCK-mCherry was present within the disrupted apicoplast vesicles. We then repeated the aforementioned growth experiment with this line in the presence of 50 μM mevalonate and 50 nM pantothenate, and observed a severe inhibition of parasite growth under the non-permissive condition (Fig 6C). Taken together, these results show that *Ec*DPCK is present and active within the disrupted apicoplast vesicles and that DPCK activity is required for parasite survival. Additionally, these results demonstrate that these vesicles remain biochemically active, as enzymes within them continue to be capable of fulfilling their essential activity.

Discussion

Plasmodium falciparum parasites rely on the supplementation of exogenous pantothenate, which is used by the parasite to generate CoA (Spry & Saliba, 2009). This process involves the cytosolic enzymes PanK1/2, PPCS1/2, PPCDC, and PPAT, while the apicoplast-localized DPCK mediates the final step (Ralph *et al,* 2004; Spry *et al,* 2008). Most of these enzymes have been targeted for deletion in *P. yoelli* or *P. berghei,* and all except for the last two (PPAT and DPCK) have proven to be dispensable for blood-stage parasite survival (Hart *et al,* 2014; Hart *et al,* 2016; Kehrer *et al,* 2016; Kenthirapalan *et al,* 2016; Srivastava *et al,* 2016; Hart *et al,* 2017). These results are largely concordant with forward genetic screens in *P. berghei* and *P. falciparum,* which suggest that DPCK is essential, and the majority of upstream enzymes in the pathway are dispensable (Schwach *et al,* 2015; Zhang *et al,* 2018) (Table 2). One notable exception is PanK1, which has been reported to be refractory to deletion in *P. falciparum* (Tjhin *et al,* 2018). The dispensability of other upstream enzymes has been attributed to the potential ability of parasites to import pantetheine, which is presumably phosphorylated by PanK1 or another kinase to generate the PPAT substrate 4′-phosphopantetheine (Hart *et al,* 2017). A similar phenomenon may explain why supplementation with CoA can bypass certain pathway inhibitors (Fletcher & Avery, 2014; Fletcher *et al,* 2016), but did not allow us to delete DPCK. If CoA cannot be imported directly into the parasite at sufficient levels, it is possible that supplemented CoA may break down into pathway intermediates, as previously reported (Spry *et al,* 2010), bypassing early pathway enzymes, but not DPCK.

While the *P. falciparum* DPCK has been predicted to be one of the few enzymes within the pantothenate pathway that is absolutely required for parasite survival, it has not been well studied. DPCK is predicted to reside within the apicoplast, performing the essential function of CoA generation for the parasite. However, the *P. falciparum* DPCK had previously neither been localized nor functionally characterized, and its essentiality had not been conclusively demonstrated. Through the work outlined here, we were able to localize DPCK to the apicoplast and show that it is essential for parasite survival. Complementation experiments confirmed that the essential activity of *P. falciparum* DPCK is shared by the previously characterized dephospho-CoA kinase (*coaE*) from *E. coli* (Mishra *et al,* 2001).

It has been shown that the apicoplast can be disrupted as long as the parasites are supplemented with IPP (Yeh & DeRisi, 2011). The disrupted apicoplast phenotype includes loss of the apicoplast genome (Gisselberg *et al,* 2013) and the presence of vesicles containing apicoplast-specific proteins (Bowman *et al,* 2014; Pasaje

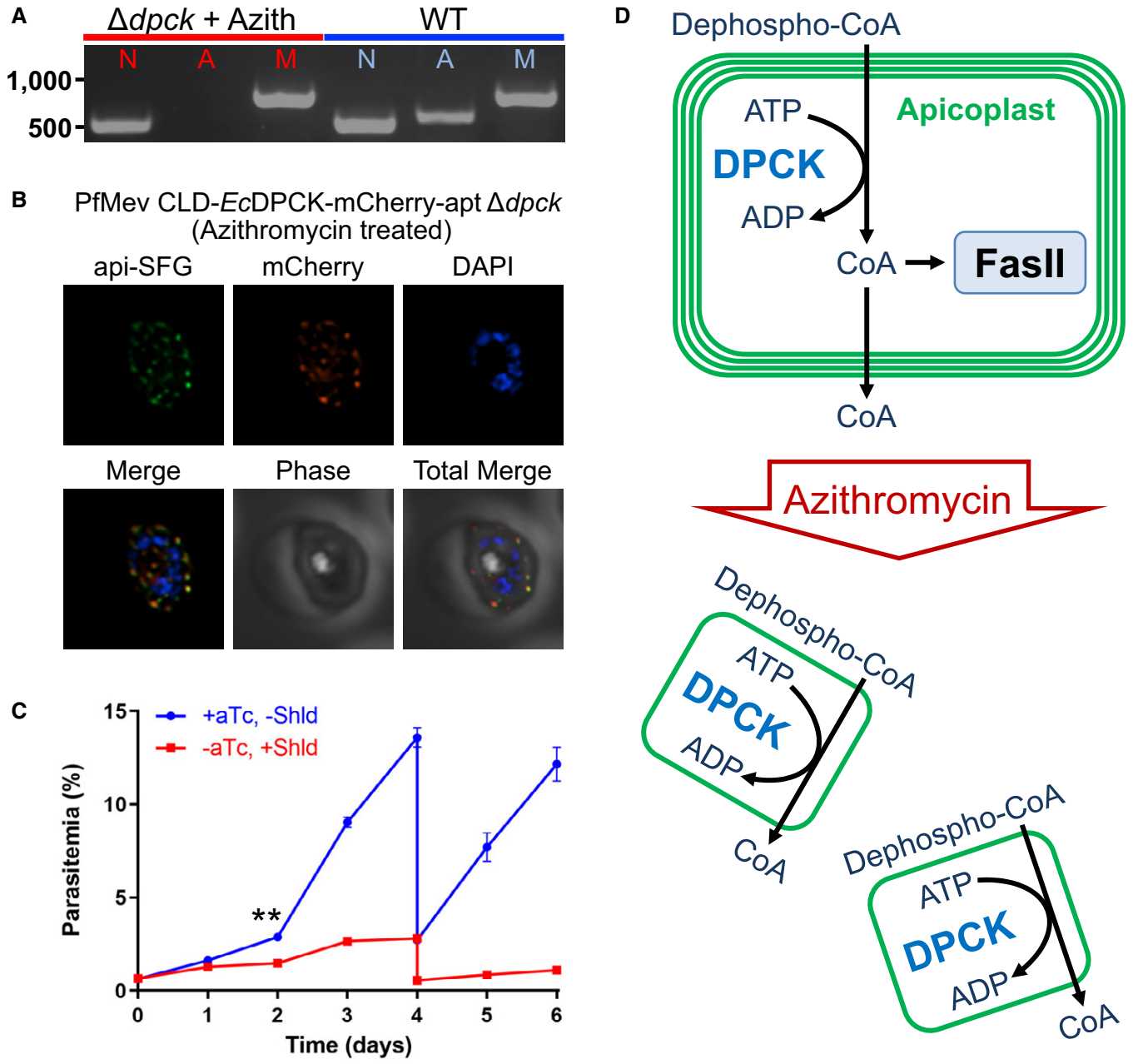

Figure 6. Characterization of azithromycin-treated PfMev CLD-*Ec*DPCK-mCherry-apt Δ*dpck* parasites under permissive and non-permissive conditions.

A Attempted PCR detection of the *ldh*, *sufB*, and *cox1* genes from the nuclear (N), apicoplast (A), and mitochondrial (M) genomes, respectively. We were unsuccessful in amplifying *sufB* from the PfMev CLD-EcDPCK-mCherry-apt Δ*dpck* parasite line after treatment with 100 nM azithromycin (Azith) in the presence of 50 μM mevalonate, indicating the disruption of the apicoplast organelle.

B Live epifluorescence microscopy of the apicoplast-negative PfMev CLD-*Ec*DPCK-mCherry-apt Δ*dpck* line post-treatment with 100 nM azithromycin in the presence of 50 μM mevalonate. This parasite line expresses api-SFG (green) and the CLD-*Ec*DPCK-mCherry construct (red) with DAPI marking the nuclei (blue). Images represent fields that are 10 μm long by 10 μm wide.

C Growth curve of the PfMev CLD-*Ec*DPCK-mCherry-apt Δ*dpck* parasite line containing a disrupted apicoplast grown either in the presence of 0.5 μM aTc and the absence 0.5 μM Shield1 (permissive condition, blue), or the absence of 0.5 μM aTc and the presence of 0.5 μM Shield1 (non-permissive condition, red). Pantothenate (50 nM) and mevalonate (50 μM) were supplied in both conditions, and the cultures were diluted 1:5 on day 4. Treatment under non-permissive conditions resulted in reduced parasite growth beginning at day 2 (two-way ANOVA, followed by Bonferroni's correction; $^{**}P < 0.01$). Error bars represent the standard error of the mean from two independent experiments, each conducted in quadruplicate.

D Upon apicoplast disruption, DPCK is located within vesicles that contain apicoplast-specific proteins and may still be able to generate CoA.

Source data are available online for this figure.

Table 2. Predicted essentiality of genes based on forward genetic screens.

	P. falciparum PiggyBac (Zhang *et al*, 2018)			*P. berghei* PlasmoGem (Schwach *et al*, 2015)	
Gene Name	**Gene ID PF3D7_#**	**Mutagenesis Index Score**	**Mutagenesis Fitness Score**	**Gene ID PBANKA_#**	**Phenotype**
PAT	0206200	1	−2.21	0303900	Not studied[a]
PanK1	1420600	0.18	−2.77	1022600	Dispensable[b]
PanK2	1437400	0.92	−2.93	0611400	Dispensable[b]
PPCS1	0412300	0.98	−2.84	0613600	Dispensable
PPCS2	1102400	1	−0.55	Absent in *P. berghei*	
PPCDC	0816100	0.16	−2.91	0714700	Dispensable
PPAT	0704700	1	−2.7	0802400	Not studied
DPCK	1443700	0.23	−3.44	1307600	Essential
ACP	0208500	0.23	−3.47	030560	Essential
ACPS	0420200	0.23	−2.64	0521600	Not studied

[a]PAT was deleted successfully in *P. berghei* (Kehrer *et al*, 2016; Kenthirapalan *et al*, 2016; Srivastava *et al*, 2016).
[b]PanK1 and PanK2 were deleted successfully in *P. berghei* (Srivastava *et al*, 2016).

et al, 2016; Florentin *et al,* 2017; Uddin *et al,* 2018). Once the apicoplast is disrupted, parasites are entirely reliant on IPP supplementation for survival (Yeh & DeRisi, 2011). From these results, it has been assumed that IPP is the only essential apicoplast product in blood-stage parasites and that parasites in this state are "apicoplast-negative", without functional apicoplast proteins and pathways. However, this conclusion is hard to reconcile with the need for CoA that is generated inside the apicoplast, as a lack of CoA should not be bypassable through IPP supplementation. Our results resolve this issue by demonstrating that DPCK cannot be bypassed by IPP because the enzyme remains functional in the vesicles remaining after apicoplast disruption.

While DPCK may still be active in disrupted apicoplast vesicles, it is important to note that continued activity is not possible for all apicoplast pathways. For instance, the apicoplast-localized MEP isoprenoid precursor pathway that is responsible for the generation of IPP (Guggisberg *et al,* 2014) would no longer be functional upon disruption, as it relies on factors encoded by the apicoplast organellar genome. Specifically, the MEP pathway relies on essential iron–sulfur (Fe-S) cluster cofactors generated by the apicoplast-localized SUF pathway, with one of the proteins within this pathway, SufB, being encoded by the organellar genome (Gisselberg *et al,* 2013). Thus, while some apicoplast-localized biochemical pathways may remain functional upon organelle disruption, this would not hold true for all pathways, especially those reliant on factors encoded by the apicoplast genome.

While the exact mechanism is unclear, DPCK can likely continue to fulfill its essential metabolic role within these vesicles if transporters within the membrane of the vesicles allow for the import of substrates and export of products (Fig 6D). In *T. gondii*, vesicles remaining after apicoplast disruption contain apicoplast membrane proteins (Tawk *et al,* 2011), suggesting that apicoplast transporters could be functional in these vesicles. Additionally, an energy source in the form of ATP is required for DPCK activity, which suggests that ATP is imported or generated by an enzyme such as pyruvate kinase II (PyrKII) in the vesicles (Ralph *et al,* 2004; Swift *et al,* 2020a). One could also further speculate that the environmental conditions (pH, redox potential, ion concentration) are also maintained in the vesicles at levels compatible with enzymatic activity.

Previous experiments using the PfMev bypass line interrogated the effect apicoplast disruption has on the parasite through the transcriptomic and metabolomic analyses of parasites containing a disrupted apicoplast and maintained on mevalonate (Swift *et al,* 2020b). These results revealed that the transcriptomic profile of parasites in this state does not appear to be meaningfully perturbed, as the nuclear transcript levels of even apicoplast-specific proteins are comparable to parasites containing an intact apicoplast (Swift *et al,* 2020b). Similarly, metabolomic experiments show that apicoplast disruption has a surprisingly small effect on metabolite levels (Swift *et al,* 2020b). These results suggest that hundreds of apicoplast-specific proteins are still generated, packaged, and sent out into the cell, but due to the disruption of the organelle, accumulate in vesicles throughout the cell. While parasites containing a disrupted apicoplast have previously been referred to as "apicoplast-negative", we have shown that the resulting vesicles remain biochemically active.

Interestingly, the expression of the cytosolic *Ec*DPCK successfully complemented the loss of the endogenous DPCK; parasites lacking apicoplast DPCK did not require mevalonate supplementation for growth or apicoplast maintenance. This suggests that CoA is not required within the apicoplast during the blood stage of the parasite. Inside the apicoplast, CoA is used to generate acetyl-CoA and malonyl-CoA (Prigge *et al,* 2003; Foth *et al,* 2005; Dellibovi-Ragheb *et al,* 2018) that feed into the FASII pathway, which has previously been shown to be dispensable in blood-stage parasites (Spalding & Prigge, 2008; Yu *et al,* 2008; Vaughan *et al,* 2009; Pei *et al,* 2010). CoA is also predicted to be used by acyl-carrier protein synthase (ACPS) to modify ACP with a 4′-phosphopantetheine modification, with the modified ACP playing a key role in the FASII pathway (Waters *et al,* 2002; Ralph *et al,* 2004; Spry *et al,* 2008; Gallagher & Prigge, 2010; Shears *et al,* 2015). While the only predicted function of ACP and ACPS within the apicoplast of *P. falciparum* parasites involves their role in the FASII pathway, both ACP and ACPS appear to be essential according to forward genetic screens in *Plasmodium* (Table 2) (Schwach *et al,* 2015; Zhang *et al,* 2018). Thus, if CoA is

indeed required within the apicoplast, it is possible that the CoA generated within the cytosol by *Ec*DPCK is imported back into the apicoplast. Presumably, there is at least one transporter that brings dephospho-CoA into the apicoplast and exports CoA during the normal operation of the apicoplast. This transporter may either be sufficiently nonspecific or possess the ability to work in reverse to bring cytosolic CoA into the organelle, thus allowing the production of CoA in the cytosol to fulfill any potential requirements within the apicoplast.

Overall, the work here demonstrates that DPCK is an essential apicoplast-localized protein that is required for parasite survival and that its function, generating CoA, cannot be bypassed with IPP. We have also shown that the vesicles derived from the disruption of the apicoplast continue to be biochemically active and capable of fulfilling essential metabolic requirements within the parasite.

Materials and Methods

P. falciparum culture and maintenance

Unless otherwise noted, blood-stage *P. falciparum* parasites were cultured in human erythrocytes at 1% hematocrit in a 10 ml total volume of CMA (Complete Medium with AlbuMAX II) containing RPMI 1640 medium with L-glutamine (USBiological Life Sciences), supplemented with 20 mM HEPES, 0.2% sodium bicarbonate, 12.5 μg/ml hypoxanthine, 5 g/l AlbuMAX II (Life Technologies), and 25 μg/ml gentamicin. Cultures were maintained in 25-cm^2 gassed flasks (94% N_2, 3% O_2, 3% CO_2) and incubated at 37°C.

Generating markerless PfMev P230p-attB parasites

A 1.2 kB region of the *p230p* gene (PF3D7_0208900) was amplified from PfMev genomic DNA using primers P230p.HA.F and P230p.HA.R (Appendix Table S2). These primers were designed to contain ~15 bp overhangs which allowed insertion of the amplicon into the NgoMIV site of pRS (Swift *et al,* 2020b) by ligation independent cloning (In-Fusion, Clontech). The plasmid was digested with BglII to excise a 210bp fragment between two BglII sites in the *p230p* gene. The excised region was replaced with an oligo comprised of complementary primers attBr. InF.F and attBr. InF.R (Appendix Table S2) using In-Fusion to generate an attB site flanked by *p230p* homology arms. The plasmid was then digested with BsaI to insert a segment of DNA encoding a guide RNA targeting the excised region of *p230p*. Complementary primers P230p.gRNA.F and P230p.gRNA.R (Appendix Table S2) were annealed and inserted using ligation independent cloning with In-Fusion (Clontech). The resulting plasmid pRS-P230p was used along with pCasG (Rajaram *et al,* 2020) in transfections for markerless insertion of the attB element into the P230p locus of PfMev parasites. After 48 h, transfectants were selected with 1.5 μM DSM1 for 7 days and 2.5 nM WR99210 for 10 days. Parasite clones were characterized by genotyping PCRs (Fig 2A) using primers described in Fig EV1 and Appendix Table S2.

Generation of the PfMev *Ec*DPCK complementation lines

The *E. coli* complementation constructs were generated from the p15-Mev-aSFG plasmid (GenBank: MN822298) containing a bidirectional Cam/HOP promoter (Swift *et al,* 2020b). On one side of the promoter, a drug resistance marker can be inserted into the BamHI/HindIII sites; on the other side, transgenes can be inserted into the AvrII/AflII sites. The plasmid also contains an attP site for integration into PfMev P230p-attB parasites (Nkrumah *et al,* 2006; Spalding *et al,* 2010). Unless noted, the construction of the complementation plasmids used ligation independent cloning with In-Fusion (Clontech).

The hDHFR drug resistance cassette was amplified from the pRS-LacZ plasmid (GenBank: MN822297) (Swift *et al,* 2020b) using the primers listed in Appendix Table S2 (hDHFR.F and hDHFR.R) and inserted into the BamHI/HindIII sites of p15-Mev-aSFG to generate p15-hDHFR. The sequence encoding *E. coli* DPCK (*Ec*DPCK) was amplified from *E. coli* genomic DNA using the primers in Appendix Table S2 (*Ec*DPCK.F and *Ec*DPCK.R) and inserted into the AvrII/BsiWI sites of the pLN-TP-ACP-mCherry plasmid (Gisselberg *et al,* 2013) to generate pLN-*Ec*DPCK-mCherry. The entire *Ec*DPCK-mCherry region was then amplified from this plasmid using the primers in Appendix Table S2 (Cam*Ec*DpmCry.F and Cam*Ec*DpmCry.R) and inserted into the AvrII/AflII sites of p15-hDHFR to generate p15-*Ec*DPCK-mCherry.

For the generation of the apicoplast-localized *E. coli* DPCK-mCherry protein, the pLN-TP-ACP-mCherry plasmid (Gisselberg *et al,* 2013) was cut with AvrII/BsiWI. The N-terminal signal and transit peptide, corresponding to the first 55 amino acids of the *P. falciparum* ACP protein (Api55), was amplified from p15-Mev-aSFG using the primers in Appendix Table S2 (pLN. Api55.F and pLN. Api55.R) and inserted upstream of the mCherry sequence to form the pLN-Api-mCherry plasmid. The sequence encoding *Ec*DPCK was then amplified from *E. coli* genomic DNA using the primers in Appendix Table S2 (Api. *Ec*DPCK.F and Api. *Ec*DPCK.R) and inserted into the BsiWI/BspEI sites of the previous plasmid. The resulting sequence, comprised of Api55, *Ec*DPCK, and mCherry, was amplified from the pLN-Api-*Ec*DPCK-mCherry plasmid using the primers in Appendix Table S2 (CamAp*Ec*DpmC.F and CamAp*Ec*DpmC.R) and then inserted into the AvrII/AflII sites of p15-hDHFR to generate p15-Api-*Ec*DPCK-mCherry.

The PfMev P230p-attB parasite line was transfected with either the p15-*Ec*DPCK-mCherry or p15-Api-*Ec*DPCK-mCherry plasmids along with the pINT plasmid encoding the bxb1 integrase (Nkrumah *et al,* 2006; Spalding *et al,* 2010). Integrants were selected for with 2.5 nM WR99210 for 7 days, after which point drug pressure was removed. Infected RBCs were then observed ~20–25 days post-transfection, at which point 2.5 nM WR99210 was added back, with the parasites maintained in the presence of this drug. Parasite lines were characterized by genotyping PCR (Fig EV2A and B) using primers listed in Appendix Table S2.

Generation of the *P. falciparum* DPCK localization line

The gene encoding *P. falciparum* DPCK (PF3D7_1443700) was amplified from cDNA using the primers (DPCK.loc.F and DPCK.loc.R) listed in Appendix Table S2 and inserted into the AvrII/BsiWI sites of p15-Api55-EcDPCK-mCherry to generate p15-*Pf*DPCK-mCherry. This plasmid was transfected into the PfMev P230p-attB parasite line along with pINT (Nkrumah *et al,* 2006; Spalding *et al,* 2010). Parasites were selected and validated as described above.

Live cell epifluorescence microscopy

Approximately 100 µl of resuspended parasite cultures was incubated with 1 µg/ml 4′, 6-diamidino-2-phenylindole (DAPI) for 30 min at 37°C. Cells were then washed three times with 100 µl of CMA medium and incubated for 5 min at 37°C after each wash. Cells were resuspended in 20 µl of CMA and then pipetted onto slides and sealed with wax for observation on a Zeiss AxioImager M2 microscope. A series of images spanning 5 µm in the z-plane were acquired with 0.2 µm spacing, and images were deconvolved using the VOLOCITY software (PerkinElmer) to report a single image in the z-plane.

Generation of *P. falciparum* plasmid constructs for gene deletion

DPCK was targeted for deletion through Cas9-mediated gene editing, using the pL8 plasmid (Swift *et al,* 2020b), in combination with the pUF1-Cas9 plasmid, which was generously provided by Dr. Jose-Juan Lopez-Rubio (Ghorbal *et al,* 2014). To generate pL8-DPCK, two DPCK homology arms (HA1 and HA2) and a 20 bp guide RNA were inserted into pL8. HA1 (562bp) was amplified with primers DPCK.HA1.F and DPCK.HA1.R, and HA2 (393bp) was amplified with primers DPCK.HA2.F and DPCK.HA2.R (Appendix Table S2). HA1 was inserted into the NotI site, and HA2 was inserted into the NgoMIV site of pL8 using In-Fusion. Primers DPCK.gRNA.F and DPCK.gRNA.R (Appendix Table S2) were annealed and inserted into the BtgZI sites of pL8 to form pL8-DPCK. For deletion of DPCK in the *Ec*DPCK complementation lines, the gene encoding hDHFR in pL8-DPCK was replaced by a codon harmonized gene encoding residues 2–129 of the *Aspergillus terreus* blasticidin-S deaminase (BSD) synthesized by LifeSct. The harmonized *bsd* gene (Appendix Fig S2) was amplified using the primers pRsBSD.F and pRsBSD.R (Appendix Table S2) and inserted into the BamHI/HindIII sites of pL8-DPCK using ligation independent cloning (In-Fusion, Clontech).

P. falciparum transfections for attempted gene deletion of DPCK

Transfections were conducted as previously described (Spalding *et al,* 2010). Briefly, 400 µl of RBCs was electroporated with 75 µg each of the Cas9 expression plasmid and the pL8-DPCK homology repair plasmid. The transfected RBCs were then mixed with synchronized schizont-stage PfMev parasites. After ~48 h, drug-selection was initiated by the addition of 1.5 µM DSM1, 2.5 nM WR99210, and 50 µM mevalonate, with or without 5 mM CoA.

Generation of the PfMev CLD-*Ec*DPCK-mCherry-apt parasite line

In order to generate the p15-CLD-*Ec*DPCK-mCherry-apt plasmid, the p15-Api-*Ec*DPCK-mCherry plasmid was digested with AvrII and BspEI in order to remove the ACP signal and transit peptide sequence. The conditional localization domain sequence was then amplified from the pLN-CLD2-HCS1 plasmid (Roberts *et al,* 2019) using the primers listed in Appendix Table S2 (CLD.F and CLD.R). The CLD-*Ec*DPCK-mCherry gene sequence was then amplified using the CLD.F and *Ec*DPCK.CLD.R primers (Appendix Table S2), and inserted into the p15-aFluc-mCh plasmid (Swift *et al,* 2020a), previously digested with AvrII and PspOMI, using In-Fusion cloning. See Appendix Fig S3 for plasmid sequence. This plasmid, along with the pINT plasmid encoding the bxb1 integrase for attP/attB integration, was transfected into p230p attB PfMev parasites and selected with 2.5 µg/ml blasticidin for 7 days, after which drug pressure was removed. Parasites were observed via Giemsa stain 20–25 days later, at which point the parasites were again cultured in the presence of 2.5 µg/ml blasticidin.

Deletion of DPCK in the PfMev *Ec*DPCK-mCherry, PfMev api-*Ec*DPCK-mCherry, and PfMev CLD-*Ec*DPCK-mCherry-apt lines

The PfMev *Ec*DPCK-mCherry and PfMev api-*Ec*DPCK-mCherry lines were transfected with the pL8-DPCK (BSD) plasmid along with the pUF1-Cas9 plasmid. The parasites were selected with 2.5 µg/ml blasticidin and 1.5 µM DSM1 for 7 days, also in the presence of 2.5 nM WR99210. After 7 days, blasticidin and DSM1 were removed. Infected RBCs were then typically seen after ~20–25 days. After parasites were observed, the cultures were then maintained in the presence of 2.5 nM WR99210 and 2.5 µg/ml blasticidin.

For the deletion of DPCK in the PfMev CLD-*Ec*DPCK-mCherry-apt parasite line, the original pL8-DPCK plasmid containing the DPCK homology arms flanking the hDHFR drug selectable marker was used. Parasites were transfected with the pL8-DPCK (hDHFR) plasmid along with the pUF1-Cas9 plasmid. Parasites were then selected with 2.5 nM WR99210 and 1.5 µM DSM1 for 7 days, also in the presence of 2.5 µg/ml blasticidin. After 7 days, WR99210 and DSM1 were removed. Infected RBCs were then typically seen after ~20–25 days. After parasites were observed, the cultures were then maintained in the presence of 2.5 nM WR99210 and 2.5 µg/ml blasticidin. Parasites were continuously cultured in the presence of 0.5 µM aTc.

Confirmation of knockout genotype

Primers were designed to screen for 5' integration (Δ5' reaction primers DPCK.5.F and pL8HA1.R) and 3' integration (Δ3' reaction primers pL8HA2.F and DPCK.3.R) of the gene disruption cassette, and the 5' region (primers DPCK.5.F and DPCK.5.WT.R) and 3' region (primers DPCK.3.WT.F and DPCK.3.R) of the WT gene (Appendix Table S2). The parental PfMev line was used as a control for these reactions.

Generation and purification of anti-mCherry rabbit antibodies

Recombinant mCherry was produced to generate affinity-purified antibodies. Primers mCh.pMAL. EcoRI. For and mCh.pMAL. HindIII. Rev (Appendix Table S2) were used to amplify mCherry for insertion into the pMALcHT *E. coli* expression vector (Muench *et al,* 2003). mCherry was expressed and purified using the same protocol previously described for the purification of recombinant GFP (Roberts *et al,* 2019). Pure recombinant mCherry was used to generate rabbit antiserum using the custom antibody service of Cocalico Biologicals Inc. Briefly, 250 µg of mCherry mixed with Complete Freund's Adjuvant was used for the initial inoculation followed by boosts of 125 µg of antigen 2, 3, and 7 weeks later. Final exsanguination was performed on day 56. Specific antibodies were purified from antiserum with a mCherry affinity column using previously described methods (Roberts *et al,* 2019). A total of 18.6 mg of anti-mCherry IgG was concentrated to 3.1 mg/ml and stored at −80°C in storage buffer (PBS, 40% glycerol, 0.02% NaN_3).

Western blotting

Parasite samples were centrifuged at 500 *g* for 5 min at room temperature (RT), and pellets were stored at −20°C until the time of protein extraction. To isolate parasites from RBCs, the pellets were thawed and resuspended in 0.15% saponin for 5 min at RT. Lysed RBCs were removed by washing three times with PBS. Parasite pellets were resuspended in NuPAGE LDS sample buffer (Thermo Fisher) containing 2% β-mercaptoethanol and incubated at 95°C for 5 min. Proteins were resolved by SDS–PAGE on 4–12% gradient gels and transferred to nitrocellulose membranes. To detect *Ec*DPCK-mCherry constructs, membranes were blocked in 5% milk and probed overnight at 4°C with 1:10,000 rabbit anti-mCherry (vide supra). They were then incubated for an hour at RT with 1:10,000 donkey anti-rabbit HRP-linked secondary antibodies (GE healthcare, NA934). Protein bands were detected on X-ray film using SuperSignal West Pico Chemiluminescent Substrate (Thermo Scientific), according to the manufacturer's protocol. Membranes were stripped of antibody with 200 mM glycine (pH 2.0) for 5 min and probed with 1:2,500 rat anti-HA mAb 3F10 (Roche) in order to detect api-SFG which contains a C-terminal HA tag (Swift *et al,* 2020b). After incubation with 1:5,000 goat anti-rat HRP-linked secondary antibodies (GE healthcare, NA935), proteins were detected as described above.

Growth curve for the PfMev CLD-*Ec*DPCK-mCherry-apt Δ*dpck* line

A culture of PfMev CLD-*Ec*DPCK-mCherry-apt Δ*dpck* parasites was washed four times with 10 ml of CMA in order to remove aTc. Parasites were then used to seed two separate 25-cm^2 flasks, each at 1% hematocrit in a 10 ml total volume of CMA media, and a starting parasitemia of ~0.5%. One flask was supplemented with 0.5 μM aTc, representing the permissive condition, while the other was treated with 0.5 μM Shield1, representing the non-permissive condition. The appropriate media were replaced approximately every 24 h, at which point a blood-film was made, and the parasitemia was determined via Giemsa stain. On day 4 of this growth curve, the parasitemia was diluted 1:10.

Pantothenate titration growth curve

Pantothenate-free media was generated, consisting of RPMI 1640 media with L-glutamine, and without pantothenate (USBiological Life Sciences #R8999-01A), supplemented with 20 mM HEPES, 0.2% sodium bicarbonate, 12.5 μg/ml hypoxanthine, 5 g/l AlbuMAX II (Life Technologies), and 25 μg/ml gentamicin. PfMev parasites were washed with 10 ml pantothenate-free media three times in order to remove the preexisting pantothenate from the culture. Parasites were then seeded into a 96-well plate at a starting parasitemia of 0.5, 2% hematocrit, and a total volume of 250 μl per well. Pantothenate was then added back to the wells containing pantothenate-free medium at a concentration of 0, 10, 50, 250 nM, or 1 μM, with CMA as a control. The appropriate media were replaced approximately every 24 h, at which point samples were collected for analysis via flow cytometry using previously described methods (Swift *et al,* 2020b). On day 4 of this growth curve, the parasitemia was diluted 1:5. In Fig EV5, error bars represent the standard error of the mean from two independent experiments, each conducted in quadruplicate.

Growth curves for the PfMev CLD-*Ec*DPCK-mCherry-apt Δ*dpck* line under limiting pantothenate concentrations

The PfMev CLD-*Ec*DPCK-mCherry-apt Δ*dpck* line was washed with 10 ml pantothenate-free media four times in order to remove aTc and pantothenate. Parasites were then seeded into a 96-well plate (Corning) at a 0.5% starting parasitemia, 2% hematocrit, and a total volume of 250 μl per well in quadruplicate. Pantothenate was added back to the pantothenate-free medium to yield a final concentration of 50 nM. Two conditions were tested: The parasites were either supplemented with 0.5 μM aTc, representing the permissive condition, or with 0.5 μM Shield1, representing the non-permissive condition. The appropriate media were replaced approximately every 24 h, at which point samples were collected for analysis via flow cytometry using previously described methods (Swift *et al,* 2020b). On day 4 of this growth curve the parasitemia was diluted 1:5. In Figs 5G and 6C, error bars represent the standard error of the mean from two independent experiments, each conducted in quadruplicate.

Inducing apicoplast loss in the PfMev api-*Ec*DPCK-mCherry Δ*dpck* and PfMev CLD-*Ec*DPCK-mCherry-apt Δ*dpck* parasite lines

The PfMev CLD-*Ec*DPCK-mCherry-apt Δ*dpck* line was cultured in media containing 100 nM azithromycin in the presence of 50 μM mevalonate for 7 days. After 7 days, the parasites were cultured continuously in the presence of 50 μM mevalonate. Loss of the apicoplast was confirmed via PCR using the methods described below.

Confirmation of apicoplast loss

The presence of the apicoplast organellar genome was detected by PCR using primers specific for the *sufB* gene (SufB.F and SufB.R). Control PCRs amplified the lactate dehydrogenase (*ldh*) gene from the nucleus (LDH.F and LDH.R) and cytochrome c oxidase subunit 1 (*cox1*) from the mitochondrial genome (Cox1.F and Cox1.R) (Appendix Table S2). For each PCR, 1 μl of parasite culture was added to a 50 μl reaction volume. The parental PfMev line was used as a positive control for apicoplast genome detection.

Data availability

This study includes no data deposited in external repositories.

Expanded View for this article is available online.

Acknowledgements
We thank Dr. Jose-Juan Lopez-Rubio for plasmid pUF1-Cas9 and Dr. Jacquin Niles for creation of the TetR-DOZI knockdown system. This work was supported by the National Institutes of Health R01 AI065853 (STP) and R21 AI101589 (STP), the Johns Hopkins Malaria Research Institute, and the Bloomberg Family Foundation. The funders had no role in study design, data collection and analysis, decision to publish, or preparation of the manuscript.

Author contributions
RPS and STP arranged the figures and wrote the manuscript, with input from all listed coauthors. RPS, HBL, and KR carried out the experiments displayed in this manuscript.

Conflict of interest

The authors declare that they have no conflict of interest.

References

Augagneur Y, Jaubert L, Schiavoni M, Pachikara N, Garg A, Usmani-Brown S, Wesolowski D, Zeller S, Ghosal A, Cornillot E *et al* (2013) Identification and functional analysis of the primary pantothenate transporter, PfPAT, of the human malaria parasite *Plasmodium falciparum*. *J Biol Chem* 288: 20558 – 20567

Bowman JD, Merino EF, Brooks CF, Striepen B, Carlier PR, Cassera MB (2014) Antiapicoplast and gametocytocidal screening to identify the mechanisms of action of compounds within the malaria box. *Antimicrob Agents Chemother* 58: 811 – 819

Crabb BS, Cowman AF (1996) Characterization of promoters and stable transfection by homologous and nonhomologous recombination in *Plasmodium falciparum*. *Proc Natl Acad Sci USA* 93: 7289 – 7294

Dellibovi-Ragheb TA, Jhun H, Goodman CD, Walters MS, Ragheb DRT, Matthews KA, Rajaram K, Mishra S, McFadden GI, Sinnis P *et al* (2018) Host biotin is required for liver stage development in malaria parasites. *Proc Natl Acad Sci USA* 115: E2604 – E2613

Epp C, Raskolnikov D, Deitsch KW (2008) A regulatable transgene expression system for cultured *Plasmodium falciparum* parasites. *Malar J* 7: 86

Fletcher S, Avery VM (2014) A novel approach for the discovery of chemically diverse anti-malarial compounds targeting the *Plasmodium falciparum* Coenzyme A synthesis pathway. *Malar J* 13: 343

Fletcher S, Lucantoni L, Sykes ML, Jones AJ, Holleran JP, Saliba KJ, Avery VM (2016) Biological characterization of chemically diverse compounds targeting the *Plasmodium falciparum* coenzyme A synthesis pathway. *Parasit Vectors* 9: 589

Florentin A, Cobb DW, Fishburn JD, Cipriano MJ, Kim PS, Fierro MA, Striepen B, Muralidharan V (2017) PfClpC is an essential Clp chaperone required for plastid integrity and Clp protease stability in *Plasmodium falciparum*. *Cell Rep* 21: 1746 – 1756

Foth BJ, Stimmler LM, Handman E, Crabb BS, Hodder AN, McFadden GI (2005) The malaria parasite *Plasmodium falciparum* has only one pyruvate dehydrogenase complex, which is located in the apicoplast. *Mol Microbiol* 55: 39 – 53

Gallagher JR, Matthews KA, Prigge ST (2011) *Plasmodium falciparum* apicoplast transit peptides are unstructured *in vitro* and during apicoplast import. *Traffic* 12: 1124 – 1138

Gallagher JR, Prigge ST (2010) *Plasmodium falciparum* acyl carrier protein crystal structures in disulfide-linked and reduced states and their prevalence during blood stage growth. *Proteins* 78: 575 – 588

Geary TG, Divo AA, Bonanni LC, Jensen JB (1985) Nutritional requirements of *Plasmodium falciparum* in culture. III. Further observations on essential nutrients and antimetabolites. *J Protozool* 32: 608 – 613

Ghorbal M, Gorman M, Macpherson CR, Martins RM, Scherf A, Lopez-Rubio JJ (2014) Genome editing in the human malaria parasite *Plasmodium falciparum* using the CRISPR-Cas9 system. *Nat Biotechnol* 32: 819 – 821

Gisselberg JE, Dellibovi-Ragheb TA, Matthews KA, Bosch G, Prigge ST (2013) The suf iron-sulfur cluster synthesis pathway is required for apicoplast maintenance in malaria parasites. *PLoS Pathog* 9: e1003655

Goldfless SJ, Wagner JC, Niles JC (2014) Versatile control of *Plasmodium falciparum* gene expression with an inducible protein-RNA interaction. *Nat Commun* 5: 5329

Guggisberg AM, Amthor RE, Odom AR (2014) Isoprenoid biosynthesis in *Plasmodium falciparum*. *Eukaryot Cell* 13: 1348 – 1359

Hart RJ, Abraham A, Aly ASI (2017) Genetic characterization of coenzyme A biosynthesis reveals essential distinctive functions during malaria parasite development in blood and mosquito. *Front Cell Infect Microbiol* 7: 260

Hart RJ, Cornillot E, Abraham A, Molina E, Nation CS, Ben Mamoun C, Aly AS (2016) Genetic characterization of Plasmodium putative pantothenate kinase genes reveals their essential role in malaria parasite transmission to the mosquito. *Sci Rep* 6: 33518

Hart RJ, Lawres L, Fritzen E, Ben Mamoun C, Aly AS (2014) *Plasmodium yoelii* vitamin B5 pantothenate transporter candidate is essential for parasite transmission to the mosquito. *Sci Rep* 4: 5665

Kehrer J, Singer M, Lemgruber L, Silva PA, Frischknecht F, Mair GR (2016) A putative small solute transporter is responsible for the secretion of G377 and TRAP-containing secretory vesicles during plasmodium gamete egress and sporozoite motility. *PLoS Pathog* 12: e1005734

Kenthirapalan S, Waters AP, Matuschewski K, Kooij TW (2016) Functional profiles of orphan membrane transporters in the life cycle of the malaria parasite. *Nat Commun* 7: 10519

Macuamule CJ, Tjhin ET, Jana CE, Barnard L, Koekemoer L, de Villiers M, Saliba KJ, Strauss E (2015) A pantetheinase-resistant pantothenamide with potent, on-target, and selective antiplasmodial activity. *Antimicrob Agents Chemother* 59: 3666 – 3668

Marin-Mogollon C, van de Vegte-Bolmer M, van Gemert G-J, van Pul FJA, Ramesar J, Othman AS, Kroeze H, Miao J, Cui L, Williamson KC *et al* (2018) The *Plasmodium falciparum* male gametocyte protein P230p, a paralog of P230, is vital for ookinete formation and mosquito transmission. *Sci Rep* 8: 14902

Mishra P, Park PK, Drueckhammer DG (2001) Identification of yacE (coaE) as the structural gene for dephosphocoenzyme A kinase in *Escherichia coli* K-12. *J Bacteriol* 183: 2774 – 2778

Muench SP, Rafferty JB, McLeod R, Rice DW, Prigge ST (2003) Expression, purification and crystallization of the *Plasmodium falciparum* enoyl reductase. *Acta Crystallogr D Biol Crystallogr* 59: 1246 – 1248

Nkrumah LJ, Muhle RA, Moura PA, Ghosh P, Hatfull GF, Jacobs Jr WR, Fidock DA (2006) Efficient site-specific integration in *Plasmodium falciparum* chromosomes mediated by mycobacteriophage Bxb1 integrase. *Nat Methods* 3: 615 – 621

Pasaje CF, Cheung V, Kennedy K, Lim EE, Baell JB, Griffin MD, Ralph SA (2016) Selective inhibition of apicoplast tryptophanyl-tRNA synthetase causes delayed death in *Plasmodium falciparum*. *Sci Rep* 6: 27531

Pei Y, Tarun AS, Vaughan AM, Herman RW, Soliman JM, Erickson-Wayman A, Kappe SH (2010) Plasmodium pyruvate dehydrogenase activity is only essential for the parasite's progression from liver infection to blood infection. *Mol Microbiol* 75: 957 – 971

Prigge ST, He X, Gerena L, Waters NC, Reynolds KA (2003) The initiating steps of a type II fatty acid synthase in *Plasmodium falciparum* are catalyzed by pfACP, pfMCAT, and pfKASIII. *Biochemistry* 42: 1160 – 1169

Rajaram K, Liu HB, Prigge ST (2020) Redesigned TetR-aptamer system to control gene expression in *Plasmodium falciparum*. *mSphere* 5: e00457-20

Ralph SA, van Dooren GG, Waller RF, Crawford MJ, Fraunholz MJ, Foth BJ, Tonkin CJ, Roos DS, McFadden GI (2004) Tropical infectious diseases: metabolic maps and functions of the *Plasmodium falciparum* apicoplast. *Nat Rev Microbiol* 2: 203 – 216

Roberts AD, Nair SC, Guerra AJ, Prigge ST (2019) Development of a conditional localization approach to control apicoplast protein trafficking in malaria parasites. *Traffic* 20: 571 – 582

Saliba KJ, Ferru I, Kirk K (2005) Provitamin B-5 (Pantothenol) inhibits growth of the intraerythrocytic malaria parasite. *Antimicrob Agents Ch* 49: 632 – 637

Saliba KJ, Kirk K (2001) H+-coupled pantothenate transport in the intracellular malaria parasite. *J Biol Chem* 276: 18115 – 18121

Schalkwijk J, Allman EL, Jansen PAM, de Vries LE, Verhoef JMJ, Jackowski S, Botman PNM, Beuckens-Schortinghuis CA, Koolen KMJ, Bolscher JM *et al* (2019) Antimalarial pantothenamide metabolites target acetyl-coenzyme A biosynthesis in *Plasmodium falciparum*. *Sci Transl Med* 11: eaas9917

Schwach F, Bushell E, Gomes AR, Anar B, Girling G, Herd C, Rayner JC, Billker O (2015) PlasmoGEM, a database supporting a community resource for large-scale experimental genetics in malaria parasites. *Nucleic Acids Res* 43: D1176 – 1182

Shears MJ, Botte CY, McFadden GI (2015) Fatty acid metabolism in the Plasmodium apicoplast: drugs, doubts and knockouts. *Mol Biochem Parasitol* 199: 34 – 50

Spalding MD, Allary M, Gallagher JR, Prigge ST (2010) Validation of a modified method for Bxb1 mycobacteriophage integrase-mediated recombination in *Plasmodium falciparum* by localization of the H-protein of the glycine cleavage complex to the mitochondrion. *Mol Biochem Parasitol* 172: 156 – 160

Spalding MD, Prigge ST (2008) Malaria pulls a FASt one. *Cell Host Microbe* 4: 509 – 511

Spry C, Chai CL, Kirk K, Saliba KJ (2005) A class of pantothenic acid analogs inhibits *Plasmodium falciparum* pantothenate kinase and represses the proliferation of malaria parasites. *Antimicrob Agents Chemother* 49: 4649 – 4657

Spry C, Kirk K, Saliba KJ (2008) Coenzyme A biosynthesis: an antimicrobial drug target. *FEMS Microbiol Rev* 32: 56 – 106

Spry C, Macuamule C, Lin Z, Virga KG, Lee RE, Strauss E, Saliba KJ (2013) Pantothenamides are potent, on-target inhibitors of *Plasmodium falciparum* growth when serum pantetheinase is inactivated. *PLoS One* 8: e54974

Spry C, Saliba KJ (2009) The human malaria parasite *Plasmodium falciparum* is not dependent on host coenzyme A biosynthesis. *J Biol Chem* 284: 24904 – 24913

Spry C, van Schalkwyk DA, Strauss E, Saliba KJ (2010) Pantothenate utilization by Plasmodium as a target for antimalarial chemotherapy. *Infect Disord Drug Targets* 10: 200 – 216

Srivastava A, Philip N, Hughes KR, Georgiou K, MacRae JI, Barrett MP, Creek DJ, McConville MJ, Waters AP (2016) Stage-specific changes in plasmodium metabolism required for differentiation and adaptation to different host and vector environments. *PLoS Pathog* 12: e1006094

Swift RP, Rajaram K, Keutcha C, Liu HB, Kwan B, Dziedzic A, Jedlicka AE, Prigge ST (2020a) The NTP generating activity of pyruvate kinase II is critical for apicoplast maintenance in *Plasmodium falciparum*. *Elife* 9: e50807

Swift RP, Rajaram K, Liu HB, Dziedzic A, Jedlicka AE, Roberts AD, Matthews KA, Jhun H, Bumpus NN, Tewari SG *et al* (2020b) A mevalonate bypass system facilitates elucidation of plastid biology in malaria parasites. *PLoS Pathog* 16: e1008316

Tawk L, Dubremetz J-F, Montcourrier P, Chicanne G, Merezegue F, Richard V, Payrastre B, Meissner M, Vial HJ, Roy C *et al* (2011) Phosphatidylinositol 3-monophosphate is involved in toxoplasma apicoplast biogenesis. *PLoS Pathog* 7: e1001286

Tjhin ET, Spry C, Sewell AL, Hoegl A, Barnard L, Sexton AE, Siddiqui G, Howieson VM, Maier AG, Creek DJ *et al* (2018) Mutations in the pantothenate kinase of *Plasmodium falciparum* confer diverse sensitivity profiles to antiplasmodial pantothenate analogues. *PLoS Pathog* 14: e1006918

Uddin T, McFadden GI, Goodman CD (2018) Validation of putative apicoplast-targeting drugs using a chemical supplementation assay in cultured human malaria parasites. *Antimicrob Agents Chemother* 62: e01161-17

van Schaijk BCL, Kumar TRS, Vos MW, Richman A, van Gemert G-J, Li T, Eappen AG, Williamson KC, Morahan BJ, Fishbaugher M *et al* (2014) Type II fatty acid biosynthesis is essential for *Plasmodium falciparum* sporozoite development in the midgut of Anopheles mosquitoes. *Eukaryot Cell* 13: 550 – 559

Vaughan AM, O'Neill MT, Tarun AS, Camargo N, Phuong TM, Aly AS, Cowman AF, Kappe SH (2009) Type II fatty acid synthesis is essential only for malaria parasite late liver stage development. *Cell Microbiol* 11: 506 – 520

Waller RF, Reed MB, Cowman AF, McFadden GI (2000) Protein trafficking to the plastid of *Plasmodium falciparum* is via the secretory pathway. *EMBO J* 19: 1794 – 1802

Waters NC, Kopydlowski KM, Guszczynski T, Wei L, Sellers P, Ferlan JT, Lee PJ, Li Z, Woodard CL, Shallom S *et al* (2002) Functional characterization of the acyl carrier protein (PfACP) and beta-ketoacyl ACP synthase III (PfKASIII) from *Plasmodium falciparum*. *Mol Biochem Parasitol* 123: 85 – 94

Yeh E, DeRisi JL (2011) Chemical rescue of malaria parasites lacking an apicoplast defines organelle function in blood-stage *Plasmodium falciparum*. *PLoS Biol* 9: e1001138

Yu M, Kumar TRS, Nkrumah LJ, Coppi A, Retzlaff S, Li CD, Kelly BJ, Moura PA, Lakshmanan V, Freundlich JS *et al* (2008) The fatty acid biosynthesis enzyme FabI plays a key role in the development of liver-stage malarial parasites. *Cell Host Microbe* 4: 567 – 578

Zhang M, Wang C, Otto TD, Oberstaller J, Liao X, Adapa SR, Udenze K, Bronner IF, Casandra D, Mayho M *et al* (2018) Uncovering the essential genes of the human malaria parasite *Plasmodium falciparum* by saturation mutagenesis. *Science* 360: eaap7847